Journal of Corrosion and Materials
www.corromat.com

J. Corros. Mater. (2026) 5(2), 211–224.

Robotic Low-Observation pH Conditioning of Buffered Electrolytes for Corrosion and Materials Chemistry

Houssein Bazzi[1,*]

Department of Chemistry and Biochemistry, Faculty of Science–Branch 1, Rafic Hariri University Campus, Lebanese University, Hadath, Lebanon

*Corresponding author: houssein.bazzi@ul.edu.lb

(Received: 3 August 2026. Received in revised form: 16 October 2026. Accepted: 28 October 2026. Published online: 30 December 2026.)

Abstract

Effective pH conditioning is an essential step prior to corrosion testing, inhibitor testing, aqueous surface treatments, aqueous cleaning, and material-degradation studies. When dealing with buffered electrolytes, the final value of pH cannot account for any historical information regarding the conditioning steps due to repeated adjustments to reach the final conditions through repeated acid-base titrations. Such manipulations may cause a different concentration, ionic strength, buffer state, and transient reaction chemistry of the solution before reaching the intended condition. This paper explores robot-assisted, low-observation, pH conditioning for buffered electrolytes prepared using acetate, citrate, ammonium, and potassium dihydrogen phosphate. Eighteen binary systems of buffer solutions at ratio 1:1, 1:2, and 2:1, along with a 4-compound electrolyte (citrate, phosphate, ammonium, and acetate), have been considered. An addition of acid or base was expressed by the titrant volume with sign. As such, only one pH meter loop could adjust the next addition based on measured pH values. Several machine learning approaches, namely linear regression, random forest regression, artificial neural network regression, and Gaussian process regression, were compared in their capability to reach the target pH range with low observation numbers. The best low-observation performance was demonstrated by Gaussian process regression, needing 3.1 ± 0.6 active observations, compared to 3.4 ± 0.3 by random forest regression and 5.6 ± 1.0 by artificial neural network regression. Adding a chemical descriptor did not have a significant effect on performance, needing 3.1 ± 0.6 active iterations with the large descriptor set and 3.2 ± 0.6 with small descriptors. Minimizing the measurement burden to only 5.8 ± 0.6 pH measurements, two initial pH values were the most suitable. Transfer learning from relevant single buffer titration history further reduced the number of active observations to 2.2 ± 0.4. Robotic experiments showed that the citrate/phosphate system needs two iterations for conditioning, the acetate/citrate systems need up to eight iterations, and a 4-compound electrolyte reaches pH 6.0 in 3.7 ± 0.4 active observations.

Keywords: buffered electrolyte; corrosion media; pH conditioning; robotic chemistry; Gaussian process regression; active learning; transfer learning; aqueous materials chemistry.

1. Introduction

Aqueous electrolyte pH plays an important role in determining the corrosion rate, inhibition efficiency, and materials degradation via several chemical reactions. Protons and hydroxides affect dissolution kinetics, hydrogen evolution reaction, hydrolysis of dissolved metal ions, stability of metal oxides and hydroxides, and oxidation states of various additives. Classical potential-pH diagrams demonstrate the pH dependence of metals, metal ions, metal oxides, and metal hydroxides in aqueous solutions [1]. General corrosion engineering texts show that practical corrosion behavior also depends on alloy condition, oxidants, aggressive ions, and surface state [2]. Electrochemical corrosion analysis further connects the observed response with kinetic and mass-transfer conditions [3]. Modern corrosion-science interpretation confirms that surface films, local chemistry, and reaction kinetics must be read together [4]. Corrosion handbook treatments provide the same practical view for engineering environments [5]. Therefore, the pH of the aqueous electrolyte is an intrinsic property of the corrosive environment itself.

Bulk pH further specifies the baseline from which local interfacial chemistry arises. The pH determined in the bulk solution does not always match the pH on the metal-solution interface where corrosion occurs. Electrochemical techniques in corrosion science show that local metal-solution conditions may diverge from the measured bulk state [6]. Corrosion-mechanism studies also emphasize the role of local interfacial reaction and transport processes [7]. Recent electrochemical texts connect these differences with migration, diffusion, hydrolysis, and accumulation of reaction products in constrained regions [8]. The processes of anodic dissolution, cathodic reduction, ion mobility, limited diffusion, hydrolysis reactions, and accumulation of corrosion products could therefore lead to localized acidification and/or alkalization in pits, crevices, coatings, surface film defects, and deposits. While a reproducible bulk value is necessary for comparative experiments, it is unable to mitigate local effects.

A standard method for pH conditioning is manually adjusting the electrolyte. An experimenter mixes in some acid or base, waits for the system to stabilize, measures the pH, and repeats the titration steps until the target pH is achieved. Although straightforward, the manual titration process may hide a chemical history of an electrolyte. Two electrolytes of equal pH might have taken different numbers of titration steps, have undergone different overshoots, have different temporary degrees of acidification and/or alkalization, have different volumes, and be in different protonation states. Ionic-equilibrium analysis shows why pH and solubility calculations depend on the complete acid-base state of the solution [9]. Aquatic-chemistry treatments further demonstrate that multi-species equilibria can alter the response to acid or base addition [10]. Electrochemical methods also require careful control of solution composition when interpreting interfacial response [11]. In particular, protonation state becomes crucial in studying inhibitors because many inhibitors are characterized by multiple acidic/basic protons and different binding properties at various pH values.

The challenge in pH adjustment is even higher for a mixture of several buffers in an electrolyte. The Henderson-Hasselbalch equation is well known for describing the titration curves of simple conjugate acid-base couples [12]. Biological-buffer design shows that multiple weak-acid and weak-base systems may be selected for different target pH regions [13]. Standard pH measurement theory also emphasizes the importance of electrode calibration and solution composition [14]. Corrosion-inhibitor and solution-chemistry studies further show that additives can change proton binding and metal interaction [15]. Thermodynamic calculations for electrolyte systems provide another basis for interpreting multi-component buffer behavior [16]. The systems studied in corrosion and materials chemistry usually include multiple weak acids, multiple weak bases, salts, complexing and passivating agents, and other compounds that affect the proton binding of the system. A mixture of carboxylates, phosphate salts, citrates, ammonium species, carbonate equilibria, and organic additives could exist within a single electrolyte system. As a consequence, the titration curve will have both flat zones with low slope, steep parts with high slopes, and curvature depending on the concentration composition. A fixed-volume manual adjustment could leave the pH unresponsive to addition of titrant in one region and result in strong overshooting in another.

Many approaches have been considered for pH regulation in continuous neutralization, water treatment, hydroponics, bioreactors, and sample preparation in analytical chemistry. Neutralization and flow-equalization studies provide a process-control background for pH adjustment [17]. Control-oriented pH-regulation studies demonstrate the nonlinear nature of neutralization processes [18]. Bioreactor and process-control work further shows that pH regulation must be treated as a feedback problem [19]. Neural and adaptive pH-control studies also support model-based adjustment strategies [20]. Additional control studies confirm the difficulty of maintaining pH in nonlinear chemical systems [21]. Live-cell culture guidance shows that pH control is also a reproducibility concern in sensitive experimental systems [22]. Automated pH-adjustment instrumentation provides an analytical-chemistry example of reducing manual preparation burden [23]. In small-volume corrosion media, pH regulation poses special challenges since every observation, every titrant addition, every mixing interval, and every electrode rinsing counts toward preparation effort. A good procedure should minimize the number of unnecessary titration steps, leaving only the essential ones, and save the titration history for future analysis.

Robotics allows to treat the pH-conditioning process as a sequence of measured actions. With the robot performing dispending of buffer stocks, addition of acid or base, mixing, pH measurements, electrode rinsing, and passing observations to a regression model, the task turns into selection of an appropriate model and finding an optimal policy for the next titration step. Active-learning theory frames this problem as choosing the next observation when each measurement carries a cost [24]. Bayesian optimization provides a related framework for efficient sequential experimentation [25]. Gaussian-process optimization has become a standard strategy for expensive black-box functions [26]. Broader reviews of Bayesian optimization further support its use in low-observation experimental settings [27]. Automated machine-learning literature also treats model and workflow selection as part of data-efficient search [28]. Machine learning in the physical sciences gives the wider basis for using data-guided decisions in scientific experiments [29]. Active experimentation in robotics demonstrated the benefits of using closed loop approach to reduce searching effort in chemical research, screening, and formulation. Robot-scientist work provided an early demonstration of automated hypothesis generation and experimentation [30]. Autonomous laboratory platforms later extended this idea to chemical search and optimization [31]. Machine-learning-guided experimental planning has also been applied to reaction optimization [32]. Robotic chemistry studies further demonstrate closed-loop molecular and formulation discovery [33]. Bayesian experimental design in reaction development supplies another example of reducing experimental effort [34].

Regression using a Gaussian process is a natural choice for modeling low-numbered observations. A Gaussian process model makes smooth predictions, can be effective with sparsely sampled data, and maintains uncertainty about the response function. Gaussian-process modelling provides a probabilistic regression framework for small datasets [35]. The standard Gaussian-process treatment also explains how prediction uncertainty is carried into interpolation and decision making [36]. Other popular non-parametric regression models such as random forest and neural network could also effectively capture nonlinear behavior. Random forests provide an ensemble-tree approach for nonlinear regression and classification [37].

Machine-learning surveys connect neural-network learning with flexible nonlinear approximation [38]. Deep-learning reviews show that neural networks may require substantial data to reach robust behavior [39]. For pH conditioning, however, the most useful prediction would not be necessarily the most accurate; the model needs to make adequate decisions about the next titration step after a couple of pH measurements.

This study explores the possibility of pH conditioning using robotics and active learning. The dataset includes 18 binary mixtures containing acetate, citrate, ammonium, and potassium dihydrogen phosphate in 1:1, 2:1, and 1:2 concentrations. The following comparison is carried out between 4 regression models, evaluation of descriptor richness, the measurement burden required to reach the target pH with 2, 3, and 4 initial measurements, transfer learning from the titration histories of similar single buffer electrolytes, and robotic performance in the binary and multi-component media. The core question that has to be considered scientifically is whether titration histories can minimize pH-conditioning efforts while providing reproducibility of the procedure through a preparative pathway for chemically diverse buffered electrolytes.

2. Materials and Methods

2.1 Buffered electrolyte media

This collection of electrolytes included eighteen buffered electrolyte media in 1:1, 1:2, and 2:1 ratios based on acetate, citrate, ammonium, and potassium dihydrogen phosphate. These media are highly chemically diverse because the chemical species involved are of importance as well as their relative abundance within each combination. Specifically, acetate forms carboxylate buffers with relatively narrow acid-base properties. The citrate system adds complexity due to the presence of multiple protonation states and relevant complexation reactions. Ammonium provides buffering capacity via weak bases. Phosphates derived from potassium dihydrogen phosphate are typical of passivation and buffering procedures.

Table 1: Binary buffered electrolytes used for robotic pH conditioning.

Index	First buffer	Second buffer	Ratio
1	Acetate	Citrate	1:1
2	Acetate	Citrate	1:2
3	Acetate	Citrate	2:1
4	Acetate	KH_2PO_4	1:1
5	Acetate	KH_2PO_4	1:2
6	Acetate	KH_2PO_4	2:1
7	Ammonium	Acetate	1:1
8	Ammonium	Acetate	1:2
9	Ammonium	Acetate	2:1
10	Ammonium	Citrate	1:1
11	Ammonium	Citrate	1:2
12	Ammonium	Citrate	2:1
13	Ammonium	KH_2PO_4	1:1
14	Ammonium	KH_2PO_4	1:2
15	Ammonium	KH_2PO_4	2:1
16	Citrate	KH_2PO_4	1:1
17	Citrate	KH_2PO_4	1:2
18	Citrate	KH_2PO_4	2:1

The numbers in Table 1 represent the full list of chemicals required for the pH control process. The ratio-based scheme is necessary since the same pair of chemicals may display varying buffering power depending on which of the two substances makes up the bulk of the solution. Acetate-citrate electrolyte of 1:2 ratio and acetate-citrate electrolyte of 2:1 ratio include the same chemicals, yet may vary in terms of titration curve slope, buffering power in target area, and risk of overshoot.

Table 2: Pair organization across buffer ratios.

Buffer pair	1:1 index	1:2 index	2:1 index
Acetate-citrate	1	2	3
Acetate-KH_2PO_4	4	5	6
Ammonium-acetate	7	8	9
Ammonium-citrate	10	11	12
Ammonium-KH_2PO_4	13	14	15
Citrate-KH_2PO_4	16	17	18

Pair-wise organization of Table 2 correlates each buffer condition with a buffer family and ratio. Pair-wise organization facilitates direct interpretation of pH-conditioning performance, since both chemical properties and stoichiometry can be identified in performance. It also enhances repeatability, since each active-learning experiment is characterized by unique buffer composition, ratio, titration data, and target pH.

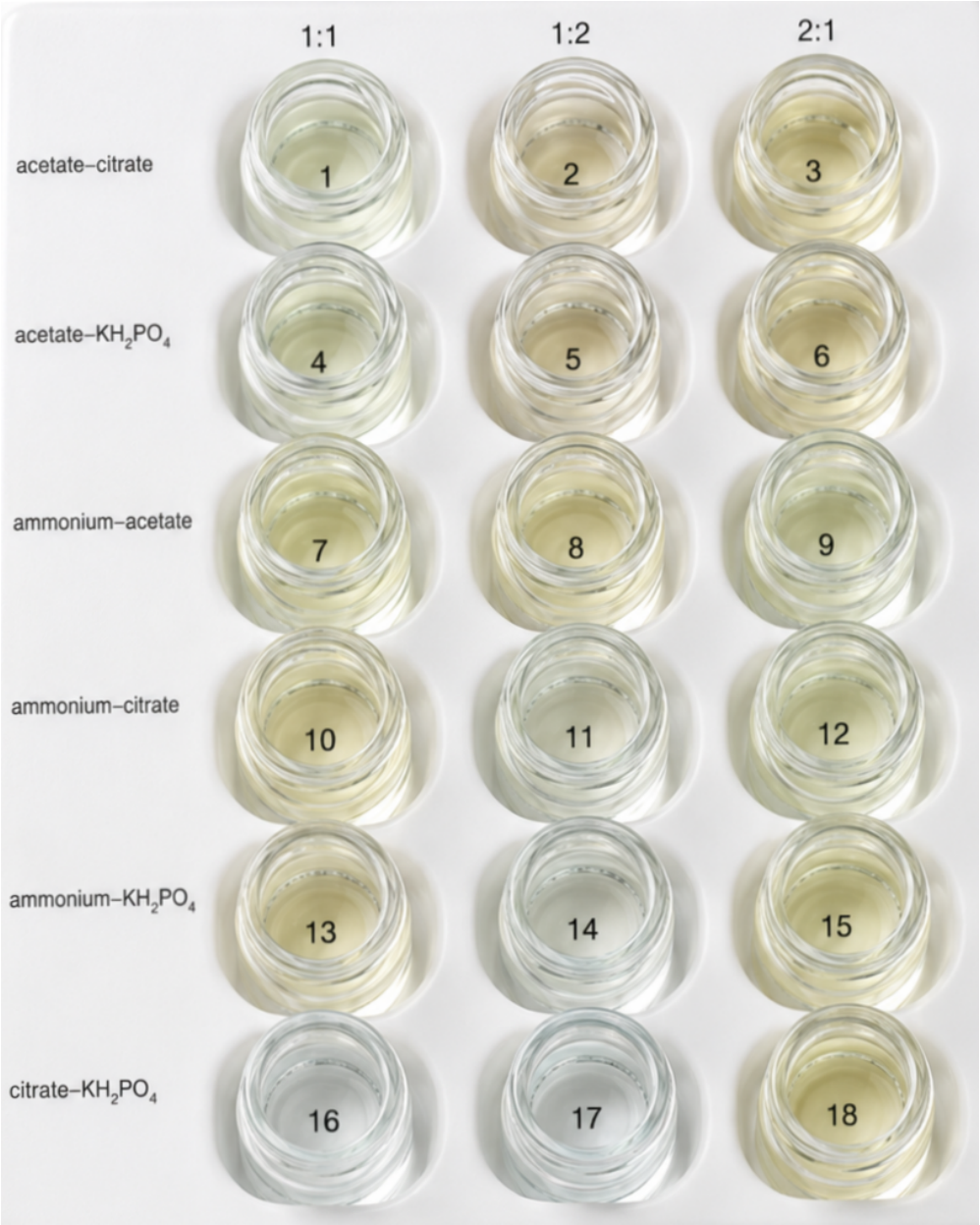

Figure 1: Binary electrolyte library.

Buffer composition rack in Figure. 1 presents the chemical inventory of the eighteen solutions prior to any robotic procedure. The three columns correspond to the buffer families at ratios 1:1, 1:2, and 2:1, respectively, while the six rows correspond to the binary buffer pairings specified in Table 2. Visual organization is essential since the active learner is assessed against a specific chemical set rather than arbitrary buffers. Ratio modification is also clearly distinguished as a parameter within the experiment rather than accidental variation between experiments.

2.2 Robotic pH-conditioning procedure

Phenomenological pH-conditioning involved a robotic workstation fitted with liquid dispensing equipment, acid and base addition, mixing, pH-measurement, and electrode cleaning. Stock buffer solutions were dispensed into glass vials using a sample wheel. Acid and base were used as titrating agents. Once mixed, sample pH was measured using the pH electrode. The pH electrode was rinsed with distilled water between pH measurements to minimize carry-over error. Controller operation and model execution were managed by a Python program.

Acid and base addition were defined using a signed titrant-volume,

$$u < 0 \quad \text{for acid addition,} \qquad u > 0 \quad \text{for base addition.} \tag{1}$$

The use of the signed-titration volume allows the controller to treat acid-base control as one-dimensional titration. Selection of a negative volume indicates that pH reduction is predicted, while selection of a positive volume predicts pH increase. One-dimensional representation eliminates dual rules for acid side and base side, giving the learner model a consistent relationship between titrant volume and pH value.

Target pH was set at 6.0 with tolerance of ±0.2 pH unit. However, in sixth electrolyte, the initial measured value lied inside the pH 6.0 interval. For this reason, target pH was set as pH 8.0. Tolerance was interpreted as laboratory acceptance interval due to the potential variability caused by pH response time, mixing duration, and buffer relaxation. A titration run was regarded as successful when measured pH fell into target band.

Figure 2: Robotic pH-conditioning station.

The figure in Fig. 2 visualizes the physical implementation of each closed-loop conditioning cycle. Central vial, pH probe, acid and base lines, rinse reservoir, and record strip visualize corresponding operations of measurement, selection, dosing, measurement, and recording observation for each cycle. Record strip is not just an interface element but also reflects the fact that each acid-base addition and measured pH must be correlated with the sample in conditioning.

Graph in Figure. 3 illustrates the signed titrant coordinate system from Eq. 1 using the measurement space of controller. Left part of axis corresponds to acid addition, while right part corresponds to base addition. Horizontal band visualizes acceptable target interval, which covers pH 5.8 to 6.2 range in our experiment. Point selected by the algorithm lies in the place where the titration response is expected to fall into target band. Visualization is useful since control problem is not equivalent to addition of predefined titrant increment, and the controller should find correct dose for the slope of the current pH response curve.

2.3 Phenomenological models and feature sets

Four regression models were used to learn titrant-volume/pH relation from active-conditioning data. Linear regression was applied as baseline model due to its assumption about linear relation between volume and pH. Random forest regression was employed since tree ensembles can approximate non-linear relationships [37]. Decision-forest analysis also supports the

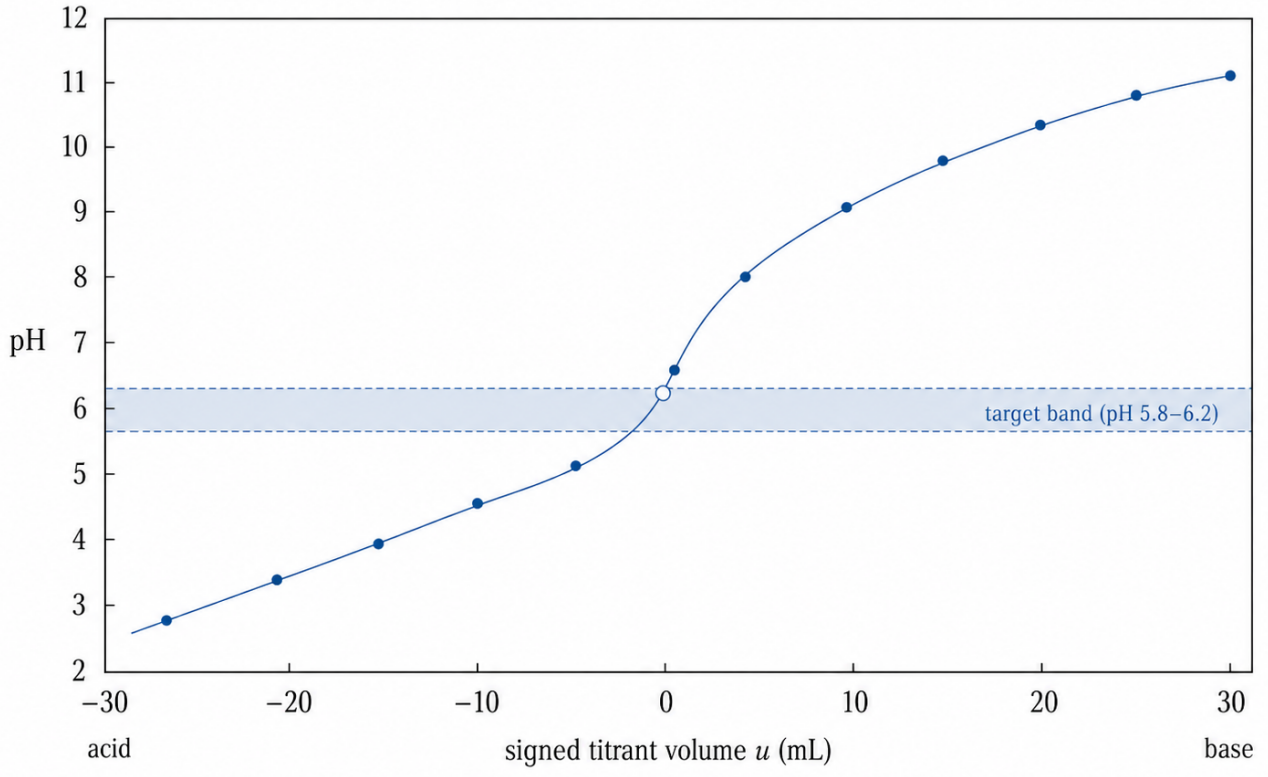

Figure 3: Signed titrant coordinate and target pH band.

use of tree ensembles for difficult nonlinear data structures [40]. Artificial neural networks can provide accurate prediction of non-linear relations if sufficient amount of training data is available [38]. Deep-learning literature also shows why neural-network flexibility may require more observations than sparse experimental designs can provide [39]. Lastly, Gaussian processes offer a convenient solution of interpolation problem for sparsely sampled points [35]. Standard Gaussian-process theory gives the uncertainty-aware regression basis for this choice [36]. Bayesian optimization work connects this model class with experimental design and sequential decision making [26].

Two sets of features were compared for all models. Larger set comprised buffer concentrations, acid and base volumes of additions, proton pKa values, total number of ionizable protons, and initial pH. Smaller set provided information regarding concentration, while excluding information on acid and base. The purpose of comparing these sets is to examine whether explicit chemical information significantly helps the model learn proper titration strategy.

For each experiment, the regression model was trained using collected data points from current experiment. Next titrant volume was predicted by selecting the point with closest predicted pH response from the allowed volume interval:

$$u_{t+1} = \arg\min_{u \in U} \left| \widehat{\mathrm{pH}}_t(u) - \mathrm{pH}^{\star} \right|. \tag{2}$$

where u_{t+1} is the next selected volume, U is the range of possible volumes, $\widehat{\mathrm{pH}}_t(u)$ is predicted response at volume u, and $\mathrm{pH}^{\star}$ is the target pH value. After the next titrant volume was tested and pH recorded, the model was trained again based on all collected data. The run ended when measured pH fell into acceptance interval.

Figure 4 illustrates Gaussian-process selection based on minimal set of data points. Mean response curve, uncertainty range, acceptance interval, and possible tick points combined allow selecting a dose prior to full mapping of titration curve. This is required for our task due to irreversible effect of each titration step on pH response curve.

2.4 Transfer learning from related buffer titrations

Transfer learning relied on pH titration data obtained from single-component buffer solutions. Transfer-learning surveys show that prior information from related tasks can reduce the learning burden in a new target task [41]. If the target binary buffer mixture contained ammonium and acetate, then single component titration history of these two components along with the initial observations on binary buffer mixture were combined. Prior history of other components was not used since it would have distorted results in a binary mixture. However, prior history served as additional knowledge which was used to train the model in advance.

The logic behind transfer learning relies on chemical similarity between single and binary mixtures. While the binary buffer mixture cannot be completely determined from the single component titration curves, they can help to estimate

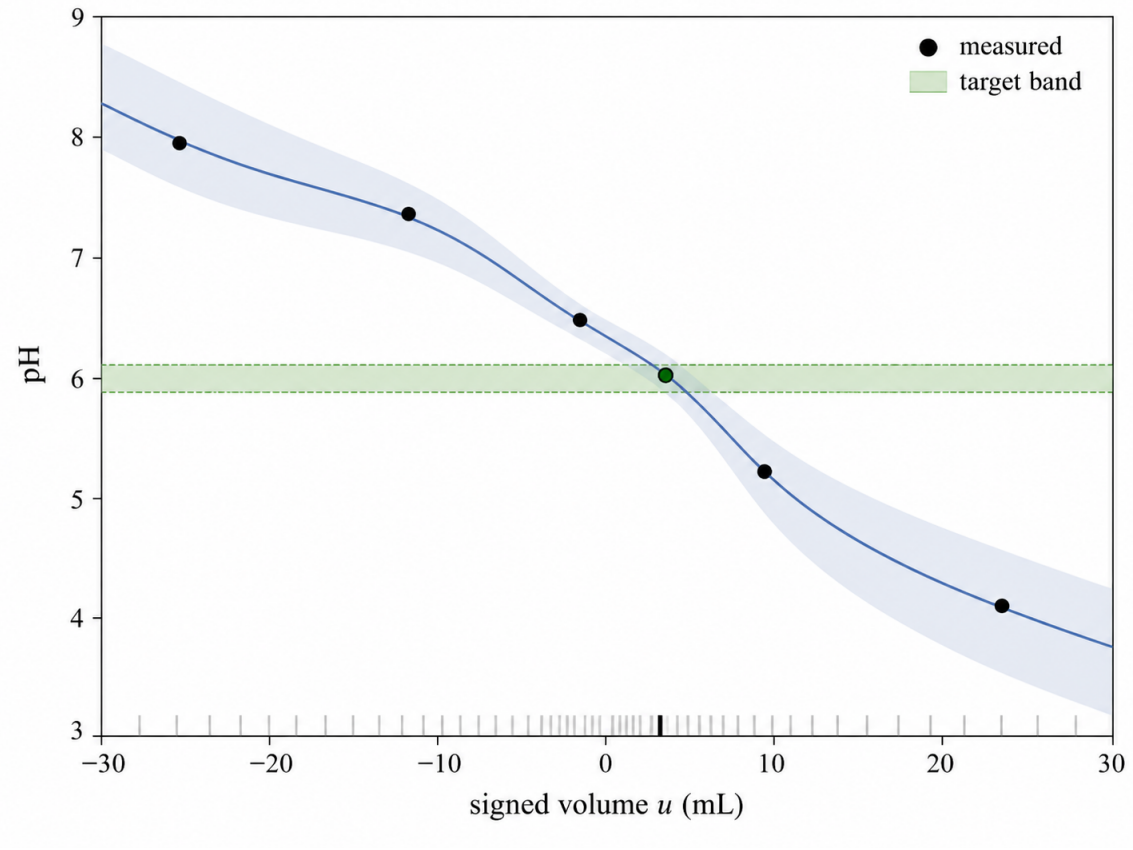

Figure 4: Gaussian-process dosing selection.

regions of rapid and slow pH changes. This might be useful for laboratories that regularly synthesize multiple electrolyte solutions.

3. Results and discussion

3.1 Electrolyte behavior

Eighteen binary electrolytes exhibited nonlinear pH response characteristic of multi-buffered acid-base mixtures. Mixtures containing citrate and phosphate generally demonstrated smooth transition due to the presence of multiple protonation stages. Ammonium- and acetate-containing mixtures demonstrated non-smooth transition due to narrower response regions of these buffers. Such distinction is crucial since electrolyte systems with close target pH values may require totally different conditioning steps.

The response of families in Figure 5 demonstrates why titrant additions of fixed volume are not reliable. In case the sample resides on a steep portion of the titration curve, even an incremental addition can drive the pH outside the target range. If the sample resides on a wide portion of the titration curve, an equal increment can induce no movement at all. In manual pH adjustment, this leads to overshooting, reverse dosing, and iterative refinement. By updating the titration relationship after each observation, automated closed-loop conditioning alleviates such issues.

For corrosion testing, the resulting nonlinear response implies that some perturbation to the initial solution could interfere with the experiment. Transient acidity can impact the rate of oxide dissolution, hydrogen evolution, and protonation of organic inhibitors. Transient basicity affects phosphate speciation, formation of hydroxyl ions, and processes of adsorption. The presence of citric acid in the media can affect metal ion coordination, while ammonium salts affect the behavior of weak bases. Thus, minimizing acid/base perturbations preserves the original electrolyte chemistry prior to introducing a test sample.

In addition, the buffer series illustrates that the degree of difficulty does not necessarily depend on the number of components in the system. While a two-component electrolyte can be more challenging to condition than a more chemically complicated one, vice versa can also be true. For example, the electrolyte composition with three components could have a more uniformly distributed buffer range. As such, measuring titration responses provides important information regardless of the nominal composition of the electrolyte.

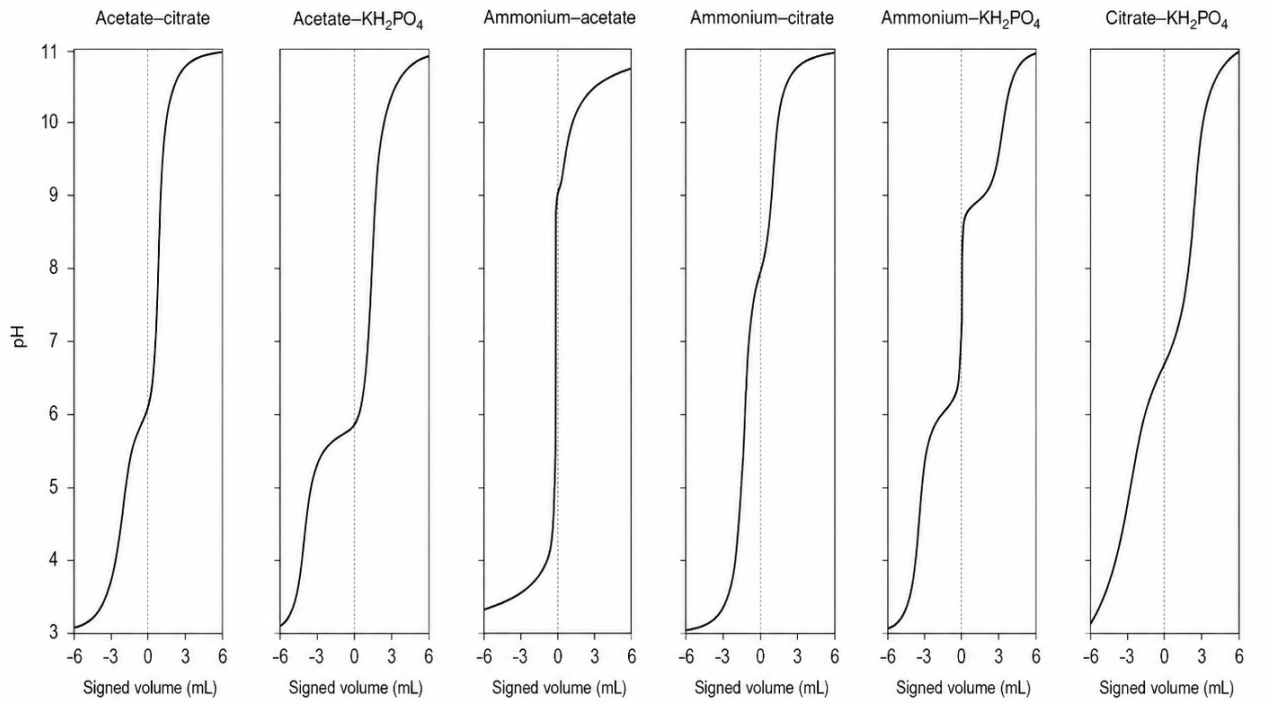

Figure 5: Buffer-family response character.

3.2 Behavior of regression models

Based on the results above, there appear to be several clear distinctions between the four regression approaches. The linear regression did not perform well because the electrolyte did not exhibit a linear dependence between the signed titrant volume and the measured pH. Complex mixtures including multistate components and multiple equilibrium systems exhibit highly nonlinear titration curves. Consequently, a linear dependence can hardly characterize a flat buffered region and a steep transition region in the same sample.

For random forest regression, the number of active iterations was 3.4 ± 0.3. It means that random forests were able to discover the nonlinearity inherent in the data using a limited number of observations. However, the main disadvantage of the random forests is that their predictions can be very stepwise. The random forests model would work well in broad-range trends prediction, but pH conditioning requires finding a particular value of the titrant.

The artificial neural networks regression model took 5.6 ± 1.0 active iterations. Even though the neural network model is capable of capturing nonlinearities, the limited number of pH measurements used during the conditioning procedure poses a challenge. The high flexibility of the neural network is counterproductive because it does not translate to the effectiveness of dosing when using few observations.

Gaussian processes regression took 3.1 ± 0.6 active iterations, showing the best average active adjustment burden. The reason behind the good performance of the Gaussian process model is interpolation between observations. A Gaussian process can learn the local properties of a titration curve from a few pH readings and use this knowledge to find a titrant volume. In small-volume corrosion electrolytes, such behavior is helpful because the solution composition changes with every adjustment.

Table 3: Active iterations required by regression models.

Regression model	Average active iterations	Observed behavior
Linear regression	Not competitive	Poor fit to nonlinear titration curves
Random forest regression	3.4 ± 0.3	Strong sparse-data response with stepwise prediction
Artificial neural network regression	5.6 ± 1.0	Nonlinear fitting with higher observation demand
Gaussian process regression	3.1 ± 0.6	Lowest active adjustment burden

The comparative cards shown in Figure. 6 give a visual comparison of Table 3. Stability under sparse observations is more critical than overall nonlinear modeling capability. While neural networks perform well as function approximators, they required many observations for the conditioning task compared to other nonlinear models. Gaussian process regression better suited the limited information due to just a few measurements. In the preparation of corrosion media, this means

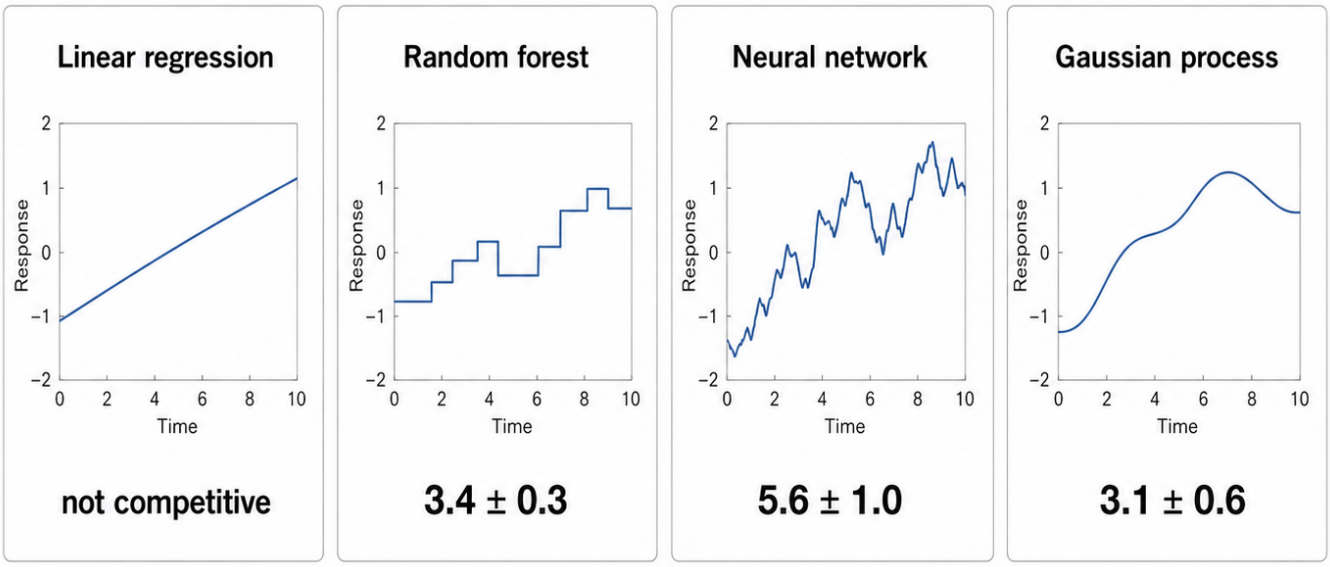

Figure 6: Regression-model control efficiency.

fewer active iterations, which decreases unwanted dilution and ionic strength shifts.

3.3 Effect of descriptor richness and response information

The descriptor effect analysis indicated that a richer chemical descriptor space provided relatively little gain. For Gaussian process regression, an increase from the lower to the higher number of descriptors increased the required number of active iterations by about 0.1 ± 0.1. This difference is negligible relative to the total variance, demonstrating that pH response obtained during conditioning contains significant control information.

Table 4: Descriptor effect in Gaussian process control.

Descriptor set	Chemical content	Average active iterations
Larger descriptor set	Concentrations, pKa values, proton counts, initial pH	3.1 ± 0.6
Smaller descriptor set	Composition and concentration information	3.2 ± 0.6

pKa values and proton counts enhance the chemical interpretation and can help to transfer to related buffer families. However, direct measurement of the response is sufficient to confirm successful buffer capacity identification. Once the first few pH measurements are completed, the slope and curvature of the response become very meaningful.

This result is valuable for practical corrosion laboratories. Most actual electrolytes include prepared compounds, cleaning agents, industrial water, or inhibitor compositions whose exact molecular makeup cannot be provided. A controller based on a complete description of the chemical features would be hard to implement. The minimal difference between the two descriptor types shows that the response-based robotized conditioning technique is feasible even with incomplete descriptors.

3.4 Initialization cost

Three initialization levels were studied: two, three, and four initial observations. The cost of the entire pH measurement was determined by the number of initialization measurements plus the amount of actively selected observations needed to meet the target band. Two initial observations led to the minimum overall cost with 5.8 ± 0.6 pH measurements. Three initial measurements resulted in 6.3 ± 0.6 observations and four in 6.8 ± 0.5.

Table 5: Total pH measurements for different initialization sizes.

Initialization size	Total pH measurements
Two initial observations	5.8 ± 0.6
Three initial observations	6.3 ± 0.6
Four initial observations	6.8 ± 0.5

The tracking plots presented in Figure. 7 prove that additional initialization does not benefit the algorithm performance. Extra initialization gives more data on how the system behaves at early stages of observation. But, along with it, the number

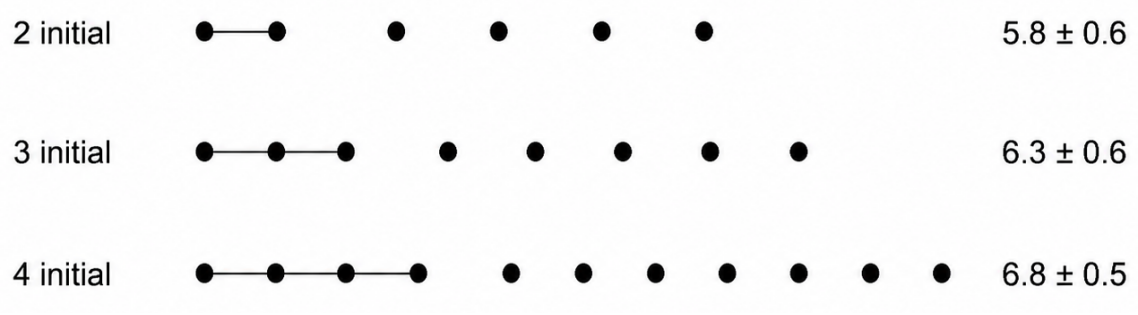

Figure 7: Initialization burden.

of measurements before active control starts also increases. In the context of the current problem, the additional information about the system did not justify itself.

Unlike complete titration, pH conditioning is a different task requiring less initialization. For mapping titration curves, initialization with more starting points would help. But for the purposes of pH conditioning with disturbance minimization, such behavior is disadvantageous. Two initialization points were sufficient for performing Gaussian process regression to enable active titrant selection.

3.5 Transfer learning with history of single buffers

Active adjustment required was reduced to a great extent by means of transfer learning. Without any history of single buffers, Gaussian process regression took 3.1 ± 0.6 iterations of adjustment. Including such information into the training phase brought the number of active iterations down to 2.2 ± 0.4.

Table 6: Transfer learning effect in Gaussian process control.

Condition	Prior titration history	Average active iterations
Without transfer learning	No related single-buffer history	3.1 ± 0.6
With transfer learning	Related single-buffer history included	2.2 ± 0.4

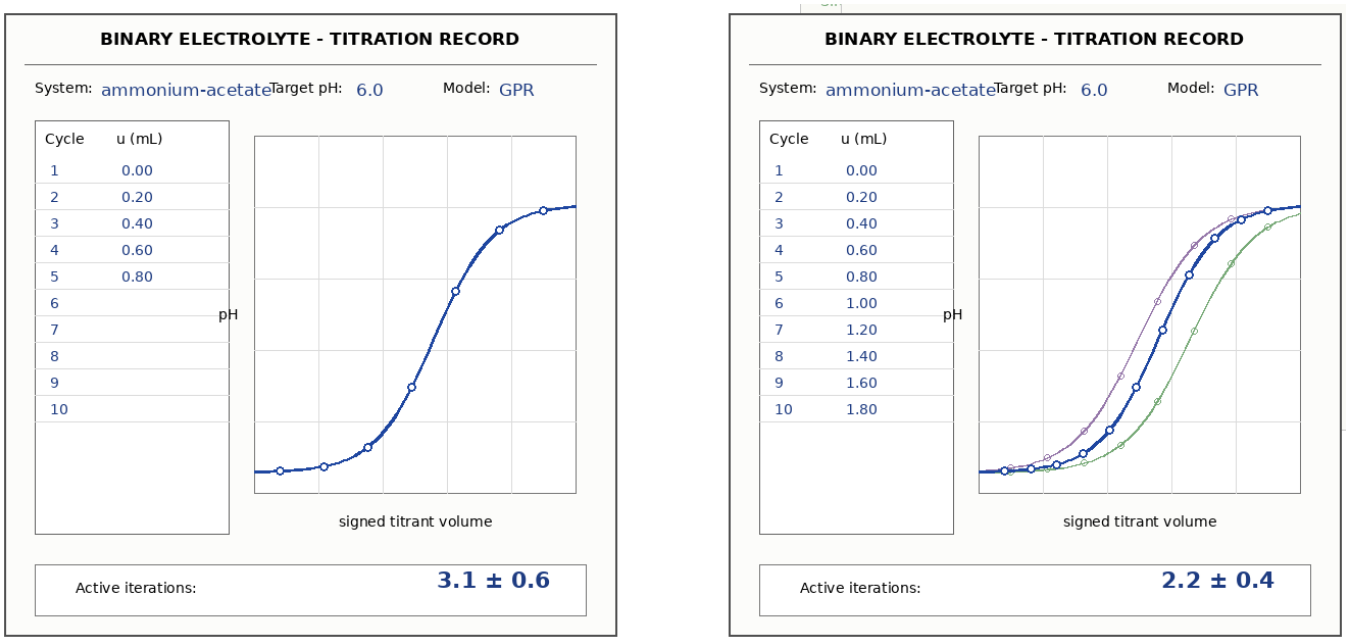

Figure 8: Transfer-learning record reuse.

The reuse of record in Figure. 8 is the practical application of Table 6. The reduction implies around 29% of the decrease in the number of active adjustment cycles:

$$\frac{3.1 - 2.2}{3.1} \times 100 \approx 29\%. \tag{3}$$

This reduction is large enough to have practical value during electrolyte preparation. One fewer cycle on average reduces the number of titrant additions, pH measurements, mixing duration, and cumulative deviation from the required composition.

The most significant gain from the transfer came for those chemically challenging binary mixtures, including the combination of ammonium and acetic acids. Such behavior stems from the more demanding nature of smaller pH buffering intervals. Having recorded the prior titration histories makes it easier for the machine learning-based model to detect whether the pH response would likely be smooth or abrupt even before performing any measurements on the newly created binary solution. The laboratory that regularly creates phosphate, citrate media, ammonium-based cleaning solutions, or carboxylate inhibitors can thus take advantage of their recorded titrations and reduce future efforts spent on electrolyte conditioning.

3.6 Validation of the algorithm using a robot for binary and four-component electrolytes

During the robotic test, we first determined the initial pH without adding titrant. Next, the controller determined the next volume of acid or base, the robot delivered it, we measured the obtained pH, and we retrained the model. We repeated this sequence until reaching the desired band of the target. The adjustment difficulty varied greatly for binary electrolytes. For example, it took only two steps for citrate-phosphate electrolytes to reach the target, and it needed as many as eight steps for acetate-citrate electrolytes.

We also tested the robotic series for a four-component electrolyte, which includes citrates, phosphates, ammonium, and acetic acids. It required 3.7 ± 0.4 steps to reach the pH 6.0 target. On average, across all experiments, it took 4.7 ± 0.4 steps.

Table 7: Robotic validation across electrolyte complexity.

Electrolyte condition	Iterations to target	Interpretation
Citrate-phosphate binary media	As few as 2	Easiest binary response
Acetate-citrate binary media	Up to 8	Most demanding binary response
Four-component citrate-phosphate-ammonium-acetate medium	3.7 ± 0.4	Successful multi-buffer conditioning
Overall robotic trials	4.7 ± 0.4	Limited-measurement operation

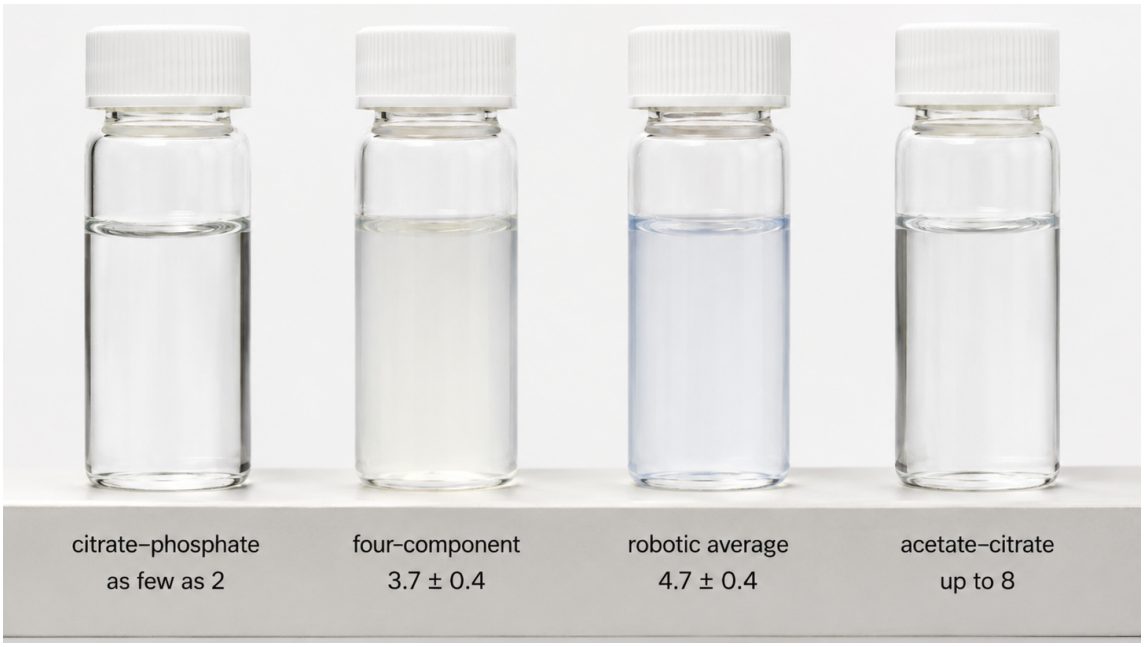

Figure 9: Robotic validation.

The validation vials presented in Figure. 9 confirm that the number of components does not determine pH conditioning complexity alone. The four-component medium took more iterations than the simplest binary medium, but less iterations than the most challenging binary medium. A binary electrolyte may be hard to condition when its target pH level falls into the area of steep pH response. On the other hand, a more chemically complex medium can respond more smoothly if its buffering capacity is distributed across the target pH interval.

This is especially significant for practical applications involving corrosion or cleaning media. Real-life solutions can contain chloride, phosphate, carbonate, citrate, ammonium, dissolved oxygen, inhibitors, surfactants, and even dissolved corrosion products. An adaptive controller that accounts for the actual measured pH response is better for dealing with

these media, in contrast to an approach that simply assumes that difficulty grows with the number of named chemical components.

3.7 Implications for corrosion and materials chemistry

The application of robotic low-observation pH conditioning significantly improves the preparation of electrolytes for corrosion and material sciences purposes in multiple chemically significant ways. First, it avoids wasteful additions of acids and bases, thus avoiding dilution and undesirable changes in ionic strength. It also registers the specific route taken to achieve the final target pH value. Moreover, it allows early titration histories to be used again if new chemically related solutions need to be prepared later.

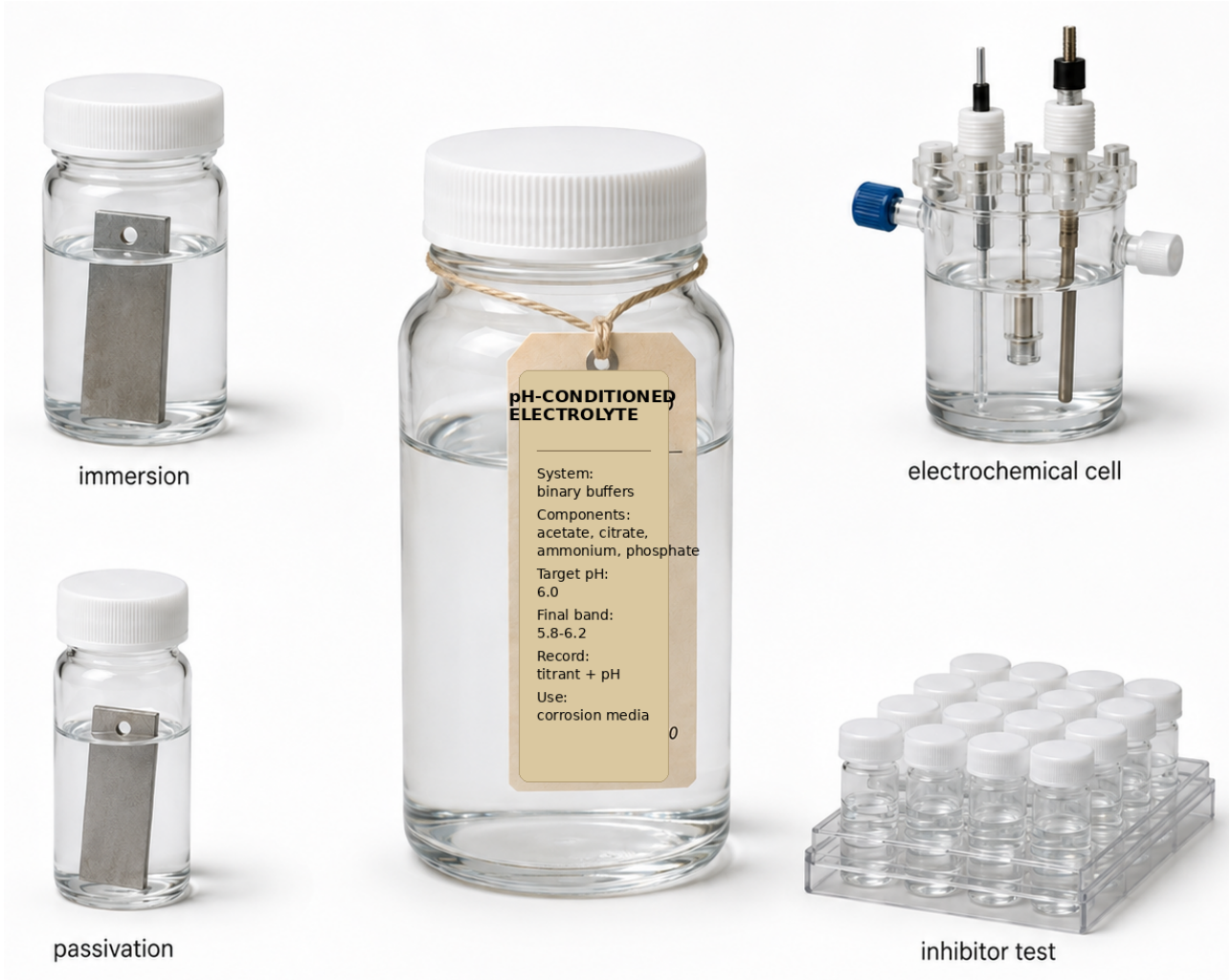

Figure 10: Preparing traceable media for corrosion testing.

The prepared medium depicted in Fig. 10 connects the concept of pH conditioning to the downstream corrosion and materials science tasks. Indeed, the very same record of the conditioned electrolyte can be used in immersion testing, electrochemical cell operations, passivation experiments, or inhibitor screening. The key point here is that the record retains pH accuracy, the number of titrants used, the number of pH observations, and the exact identity of the prepared media.

These properties make the method highly relevant to immersion testing, electrochemical polarization, impedance spectroscopy, inhibitor screening, surface passivation, aqueous material degradation studies, and cleaning bath evaluation. In all cases, the pH plays an important role in determining the properties of the solution and the reaction of its interface with metals. If pH is manually achieved by uncontrolled means, discrepancies between samples may stem from different preparation history, while recording and optimizing it would eliminate these sources of error.

The proposed method is highly valuable for evaluating organic inhibitors. They can shift their protonation state depending on pH, and adsorb differently on metal oxides and hydroxides depending on the sign of charge and local solution chemistry. Phosphate-containing electrolytes can serve for passivation purposes but may respond sharply to changes in pH. Citrate-containing solutions can alter the speciation of metal ions, while ammonia solutions can shift weak-base equilibrium constants. A robotic method that achieves the target pH through minimum disturbances would allow for maintaining the

desired chemical conditions until the start of corrosion tests.

The additional evidence of the method's utility comes from the experiment on descriptors' comparison. A full list of descriptors describing acids/bases cannot always be available in applied laboratories. On the other hand, measured pH response gives just enough information for effective control after just a few measurements. Thus, the method proves useful not only for perfectly described model electrolytes but also for common laboratory solutions.

Mixture identity: *Binary buffered electrolyte (B1)*

Target pH: *6.0* Target band: *5.8 – 6.2* Model used: *Gaussian process*

Step	Initial pH (at step start)	Titrant addition (mL) (+ NaOH / – HCl)	Measured pH (at step end)	Model used	Target band	Accepted endpoint?
0	5.24	0.00	5.24	Gaussian process	5.8 – 6.2	–
1	5.24	+ 0.40	5.56	Gaussian process	5.8 – 6.2	–
2	5.56	+ 0.30	5.80	Gaussian process	5.8 – 6.2	–
3	5.80	+ 0.10	5.92	Gaussian process	5.8 – 6.2	–
4	5.92	+ 0.05	5.98	Gaussian process	5.8 – 6.2	–
5	5.98	+ 0.03	6.01	Gaussian process	5.8 – 6.2	–
6	6.01	– 0.01	6.00	Gaussian process	5.8 – 6.2	inside band

Notes: *Endpoint accepted: pH 6.00 is inside target band 5.8 – 6.2.*

Figure 11: A record sheet per single conditioning run.

The sample record sheet in Figure. 11 shows the increased reproducibility of the method. A full conditioning process includes identification of the solution, target pH value, target band, signed titrant sequence used, measured pH values, regression model, and decision criteria for termination. Unlike just reporting a target pH value, this detailed record describes the precise chemical route along which the target band was achieved. Such kind of route-level record is especially valuable if the same electrolyte family needs to be prepared again, but slightly differently, e.g., by changing concentrations of inhibitors or the buffer identity.

4. Conclusions

A novel approach to the preparation of buffered electrolytes through pH conditioning using a robotic platform and Gaussian process regression proved highly promising. The study examined a set of eighteen binary mixtures of acetate, citrate, ammonium, and potassium dihydrogen phosphate in 1:1, 1:2, and 2:1 ratios. Their non-linear titration behavior was the source of difficulty of fixed-increment adjustments and prevented any usage of linear regression for the control.

Among all models, Gaussian process regression had the smallest number of active pH conditioning iterations at 3.1 ± 0.6. Random forest regression showed comparable results (3.4 ± 0.3 active pH-conditioning steps), however, predicted step-wise pH response. Artificial neural networks took 5.6 ± 1.0 steps, proving ineffectiveness of purely high flexibility without sufficient observation.

Enrichment of descriptors led to the small gain of efficiency, 3.1 ± 0.6 active iterations for the big set and 3.2 ± 0.6 for the small one. This confirmed that direct pH titration response obtained during pH conditioning gives enough information for making dosing decisions. The best number of pH measurements used in two-point initialization resulted in 5.8 ± 0.6 steps in average. Transfer learning from the history of similar single buffer reduced the number of active steps to 2.2 ± 0.4, i.e., roughly 29% fewer steps.

The robotic pH validation demonstrated the achievement of target pH in citrate-phosphate binary electrolytes in 2 active steps; citrate-acetate binary media took up to 8 active steps, while four-component citrate-phosphate-ammonium-acetate electrolyte reached pH 6.0 in 3.7 ± 0.4 iterations. Therefore, pH-conditioning difficulty can largely depend on actual pH response.

The principal benefit of the developed technique is the opportunity to control pH preparation route. Fewer additions reduce dilution, avoid ionic strength drift, and prevent transient solution chemistry. The recorded titration histories also become more valuable since they can be reused to condition the subsequent chemically-related electrolyte families. Thus, pH conditioning based on robotic titration and regression can be successfully used in corrosion tests, organic inhibitors screening, surface passivation, cleaning baths development, degradation studies, and formulation work.

Conflict of Interest

The author declares no conflict of interest.

References

[1] Pourbaix, M. (1974). Atlas of electrochemical equilibria in aqueous solutions. (No Title).
[2] Jones, D. A. (1996). Principles and prevention of corrosion. (No Title).
[3] Landolt, D. (2007). Corrosion and surface chemistry of metals. EPFL press.
[4] McCafferty, E. (2010). Introduction to corrosion science. Springer Science & Business Media.
[5] Revie, R. W. (Ed.). (2011). Uhlig's corrosion handbook. John Wiley & Sons.
[6] Kelly, R. G., Scully, J. R., Shoesmith, D., & Buchheit, R. G. (2002). Electrochemical techniques in corrosion science and engineering. CRC press.
[7] Marcus, P., & Oudar, J. (Eds.). (2002). Corrosion mechanisms in theory and practice (pp. 243-286). New York: Marcel Dekker.
[8] Monteiro, H. B., & Tartakovsky, D. M. (2026). Integral Kernel Methods for Nonlinear Parabolic-Elliptic Systems. SIAM Journal on Scientific Computing, 48(2), A958-A983.
[9] Butler, J. N. (1998). Ionic equilibrium: solubility and pH calculations. John Wiley & Sons.
[10] Stumm, W., & Morgan, J. J. (2013). Aquatic chemistry: chemical equilibria and rates in natural waters. John Wiley & Sons.
[11] Bard, A. J., Faulkner, L. R., & White, H. S. (2022). Electrochemical methods: fundamentals and applications. John Wiley & Sons.
[12] Hasselbalch, K. A. (1916). Die Berechnung der Wasserstoffzahl des Blutes aus der freien und gebundenen Kohlensäure desselben, und die Sauerstoffbindung des Blutes als Funktion der Wasserstoffzahl. Julius Springer.
[13] Good, N. E., Winget, G. D., Winter, W., Connolly, T. N., Izawa, S., & Singh, R. M. (1966). Hydrogen ion buffers for biological research. biochemistry, 5(2), 467-477.
[14] Bates, R. G. (1964). Determination of pH: theory and practice.
[15] Nguyen, M. K., Kao, L., & Kurtz, I. (2009). Calculation of the equilibrium pH in a multiple-buffered aqueous solution based on partitioning of proton buffering: a new predictive formula. American Journal of Physiology-Renal Physiology, 296(6), F1521-F1529.
[16] Brown, P. L., & Ekberg, C. (2016). Hydrolysis of Metal Ions. Wiley.
[17] Goel, R. K., Flora, J. R., & Chen, J. P. (2005). Flow equalization and neutralization. In Physicochemical treatment processes (pp. 21-45). Totowa, NJ: Humana Press.
[18] Tan, W. W., Lu, F., Loh, A. P., & Tan, K. C. (2005). Modeling and control of a pilot pH plant using genetic algorithm. Engineering Applications of Artificial Intelligence, 18(4), 485-494.
[19] Åkesson, B. M., Toivonen, H. T., Waller, J. B., & Nyström, R. H. (2005). Neural network approximation of a nonlinear model predictive controller applied to a pH neutralization process. Computers & chemical engineering, 29(2), 323-335.
[20] Altınten, A. (2007). Generalized predictive control applied to a pH neutralization process. Computers & chemical engineering, 31(10), 1199-1204.
[21] Alwan, G. M. (2008). pH-control Problems of wastewater treatment plants. Al-Khwarizmi Engineering Journal, 4(2), 37-45.
[22] Michl, J., Park, K. C., & Swietach, P. (2019). Evidence-based guidelines for controlling pH in mammalian live-cell culture systems. Communications biology, 2(1), 144.
[23] Zhu, Y., Nishigori, S., Shimura, N., Nara, T., & Fujimori, E. (2020). Development of an automatic pH adjustment instrument for the preparation of analytical samples prior to solid phase extraction. Analytical Sciences, 36(5), 621-625.
[24] Settles, B. (2009). Active learning literature survey.
[25] Brochu, E., Cora, V. M., & De Freitas, N. (2010). A tutorial on Bayesian optimization of expensive cost functions, with application to active user modeling and hierarchical reinforcement learning. arXiv preprint arXiv:1012.2599.
[26] Snoek, J., Larochelle, H., & Adams, R. P. (2012). Practical bayesian optimization of machine learning algorithms. Advances in neural information processing systems, 25.
[27] Shahriari, B., Swersky, K., Wang, Z., Adams, R. P., & De Freitas, N. (2015). Taking the human out of the loop: A review of Bayesian optimization. Proceedings of the IEEE, 104(1), 148-175.
[28] Hutter, F., Kotthoff, L., & Vanschoren, J. (2019). Automated machine learning: methods, systems, challenges. Springer.
[29] Carleo, G., Cirac, I., Cranmer, K., Daudet, L., Schuld, M., Tishby, N., ... & Zdeborová, L. (2019). Machine learning and the physical sciences. Reviews of Modern Physics, 91(4), 045002.
[30] King, R. D., Whelan, K. E., Jones, F. M., Reiser, P. G., Bryant, C. H., Muggleton, S. H., ... & Oliver, S. G. (2004). Functional genomic hypothesis generation and experimentation by a robot scientist. Nature, 427(6971), 247-252.
[31] Burger, B., Maffettone, P. M., Gusev, V. V., Aitchison, C. M., Bai, Y., Wang, X., ... & Cooper, A. I. (2020). A mobile robotic chemist. Nature, 583(7815), 237-241.
[32] Eyke, N. S., Green, W. H., & Jensen, K. F. (2020). Iterative experimental design based on active machine learning reduces the experimental burden associated with reaction screening. Reaction Chemistry & Engineering, 5(10), 1963-1972.
[33] Cao, L., Russo, D., Felton, K., Salley, D., Sharma, A., Keenan, G., ... & Lapkin, A. A. (2021). Optimization of formulations using robotic experiments driven by machine learning DoE. Cell Reports Physical Science, 2(1).
[34] Shields, B. J., Stevens, J., Li, J., Parasram, M., Damani, F., Alvarado, J. I. M., ... & Doyle, A. G. (2021). Bayesian reaction optimization as a tool for chemical synthesis. Nature, 590(7844), 89-96.
[35] Seeger, M. (2004). Gaussian processes for machine learning. International journal of neural systems, 14(02), 69-106.
[36] Rasmussen, C. E., & Williams, C. (2006). Gaussian processes for machine learning the mit press. Cambridge, MA, 32, 68.
[37] Breiman, L. (2001). Random forests. Machine learning, 45(1), 5-32.
[38] Jordan, M. I., & Mitchell, T. M. (2015). Machine learning: Trends, perspectives, and prospects. Science, 349(6245), 255-260.
[39] Schmidhuber, J. (2015). Deep learning in neural networks: An overview. Neural networks, 61, 85-117.
[40] Ho, T. K. (2002). A data complexity analysis of comparative advantages of decision forest constructors. Pattern Analysis & Applications, 5(2), 102-112.
[41] Pan, S. J., & Yang, Q. (2009). A survey on transfer learning. IEEE Transactions on knowledge and data engineering, 22(10), 1345-1359.